Online Estimation of Engine Driveline Dynamic Properties

M. Madamedon, F. Gu, A. Aburass and A.D Ball
Centre for Efficiency and Performance Engineering (CEPE), University of Huddersfield,
U0973878@hud.ac.uk

Abstract—This paper investigates the dynamics of the engine driveline system for achieving accurate and online diagnostics of engine conditions using instantaneous angular speed (IAS). Based on a state space modelling approach and key structures of the system, a torsional vibration model is developed and its modal properties: modal frequency, damping ratio and shapes are evaluated. Then taking the output data from the model as the input a latest stochastic subspace identification (SSI) method was implemented and result shows that the SSI approach is sufficiently accurate to extract these modal properties. Moreover, experimental studies show that the SSI approach can correctly extract modal properties under the low frequency range of interest based on just the transient IAS data acquired during engine shutdown, which confirms the theoretical analysis and provides the basis for the subsequent IAS based diagnosis development in which modal characteristics will be taken into account.

Keywords—Instantaneous angular speed; modal identification; Output only modal identification; SSI

I. INTRODUCTION

Over the years IAS measurement of diesel engines has shown a close relation to the gas pressure and power torque acting on the crankshaft. Hence, its analyses have shown good prospects in the diagnosis of combustion related faults and other faults that affect gas pressure [5]. Current methods have been classified into statistical estimator, pattern recognition and order domain methods or a combination of any of these methods [12, 13].

While the group of statistical estimator and pattern recognition techniques rely mainly on the measured IAS data to detect faults, order domain or model based deconvolution techniques rely on the use of the engine driveline model developed by [14] to reconstruct the applied torque and cylinder pressure contribution of each cylinder from measured IAS data. Citron et al. [15] using an elastic model of the engine-Drivetrain was able to pass back through the model, measured IAS data to extract the engine torque fluctuation waveform and from it the engine pressure, torque fluctuation waveform, whose non-uniformity then provided the basis for assessing cylinder to cylinder pressure waveform and combustion variability.

Using the rigid body crankshaft model [13] was able to detect power imbalance in a multi-cylinder inline diesel engine and identified faulty cylinders by analyzing lower harmonic orders which allowed the speed variation spectrum to filter out the distortions produced by the dynamic response of the crankshaft.

The aim of IAS diagnostics based on model deconvolution is to use the measured torsional vibration signature, i.e. the measured IAS, to gain precise insight into the characteristics of the forcing torque generated by different cylinders, which relates to the individual cylinder pressure contribution and reflects its combustion performance.

Hence, in order to gain insight into the individual cylinder pressure waveform from measured IAS data it is vital to accurately determine structural driveline modal parameters [16].

Despite this, IAS diagnostics based on model deconvolution which account for torsional modal properties (frequency, damping and modal vectors) has been less studied.

Thus, this paper focuses on the use of IAS response for performing an output only modal identification. Firstly, a torsional vibration state space model which takes into consideration the flexible coupling between engine and dynamometer was developed and the modal parameters evaluated. Then a pseudo random input was used in exciting the system and the response passed through the SSI approach and the result compared with the theoretical calculated ones.

Consequently, the SSI algorithm was implemented using IAS response during the engine's transient shut down operations.

II. MODEL OF ENGINE SYSTEM

Through a crank-slider mechanism the rectilinear movement of the piston is transformed into rotation of the crankshaft [7]. Figure 1 below depicts the connection between the piston and the crankthrow via the connecting rod. According to [8], the connecting rod can be assumed to be a rigid body while the joints at A (the piston pin) and B (the crank pin) are assumed to be free of clearance.

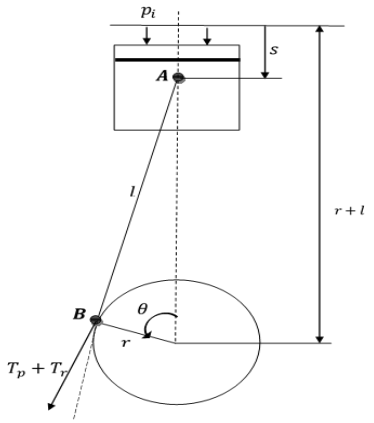

Figure 1 crank-slider mechanism

p_i, is the cylinder pressure
r, is the crank radius
l, is the connecting rod length
s, is the engine stroke
θ, is the crank angle
T_p, is the torque resulting from the gas pressure
T_r, is the torque due the reciprocating inertia
The total torque acting on the crankthrow is $=T_p + T_r + T_f$.
T_f, is the torque due to friction.

A. The Engine-Drive Model

For real time applications, there is an incentive for reducing the model complexity [8]. In this paper the approach where the lumps with cylinders connected are condensed is considered. Hence, the model in effect becomes a single cylinder multi-firing model with the flywheel end of the crankshaft and the load modelled as individual inertia lumps, thus, are able to handle crankshaft deformations.
Figure 3 below shows the three degrees of freedom torsional vibration model.

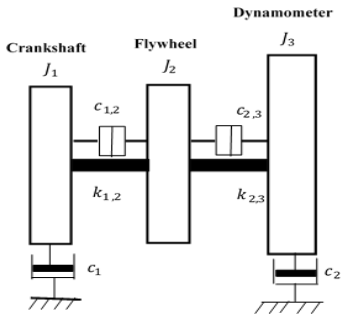

Figure 3 engine driveline system model

B. State Space Modelling of Engine Driveline System

A discrete mechanical system such as the engine driveline system, having n masses connected through springs and dampers behaves dynamically according to the following matrix differential equation [6, 11]:

$$M\ddot{U}(t) + C_2\dot{U}(t) + KU(t) = F(t) = B_2u(t) \quad (1)$$

M, C_2, K, are mass, damping and stiffness matrix. $F(t)$, is the excitation force factorized into a matrix B_2 which describes the input in space and a vector $u(t)$ which describes it in time. U, is the displacement vector at continuous time t. This can be defined in a continuous time state space model as:

$$\dot{x}(t) = A_cx(t) + B_cu(t)$$
$$y(t) = Cx(t) + Du(t) \quad (2)$$

$x, \dot{x}$, are system input and its derivative
y, is the system output
u, is input to the combined system

$A = \begin{bmatrix} 0 & 1 \\ -M^{-1}K & -M^{-1}C_c \end{bmatrix}$, is the system matrix, inertia matrix $M = \begin{bmatrix} J_1 & 0 & 0 \\ 0 & J_2 & 0 \\ 0 & 0 & J_3 \end{bmatrix}$, stiffness matrix $K = \begin{bmatrix} k_1 & -k_1 & 0 \\ -k_1 & k_1 + k_2 & k_2 \\ 0 & -k_2 & k_2 \end{bmatrix}$, and damping matrix $C_c = \begin{bmatrix} c_1 & -c_1 & 0 \\ -c_1 & c_1 + c_2 & c_2 \\ 0 & -c_2 & c_2 \end{bmatrix}$,
$B_c(t) = \begin{Bmatrix} 0 \\ M^{-1}T(t) \end{Bmatrix}$, is the input matrix.

Friction torque is modelled as viscous absolute damping elements and therefore incorporated in the damping matrix C hence, consequential $T_f(\theta) = 0$.
The excitation torque, which actuates each crank throw is then the sum of the torque due to reciprocating inertia and the torque due to gas pressure on that crank throw.

$T_e(\theta)i = T_p(\theta)i + T_r(\theta)i;\ i = 1{:}\,4$ (depending on the number of cylinders). The excitation vector is:

$$T(t) = (T_e i \quad 0 \quad \cdots \quad T_l)^T \quad (3)$$

C, is the output matrix
D, is the feedback matrix (zero in case of mechanical systems).
After sampling the discrete time state space model is:

$$x_{k+1} = Ax_k + Bu_k$$
$$y_k = Cx_k + Du_k \quad (4)$$

$x_k = x(k\Delta t)$, is the discrete-time vector, $A = \exp(A_c\Delta t)$ is the discrete state matrix and $B = [A \ -I]A_c^{-1}B_c$, is the discrete input matrix.
Adding the stochastic components the discrete-time combined deterministic-stochastic state-space model [11] is:

$$x_{k+1} = Ax_k + Bu_k + w_k$$
$$y_k = Cx_k + Du_k + v_k \quad (5)$$

w_k, is the process noise due to disturbance and modelling inaccuracies and v_k, is measurement noise due to sensor inaccuracy. Both are immeasurable and are assumed to be a white noise with a zero mean, having covariance matrices [11]:

$$E\left[\begin{pmatrix} w_p \\ v_p \end{pmatrix}\begin{pmatrix} w_q^T & v_q^T \end{pmatrix} = \begin{pmatrix} Q & S \\ S^T & R \end{pmatrix}_{\delta_{pq}}\right] \quad (6)$$

E, is the expected value operator and δ_{pq}, is Kronecker delta.

C. Modal Properties

In order to study the engine-dynamometer system under transient operations a state space model was formulated in

Matlab. The engine's key driveline parameters used for the simulation is shown in Table 1

Table 1 key Driveline parameters used for Engine transient operation simulations.

J_1	0.2255kg. m^2
J_2	(0.4060+2.4741)= 2.8801 kg. m^2
J_3	0.3800kg. m^2
$c_{1,2}$	0.009
$c_{2,3}$	0.122
$k_{1,2}$	1.1706e6N/rad
$k_{2,3}$	2.25e3Nm /rad

The modal parameters: modal frequencies, damping ratio and shapes obtained by solving Eig equation based on known driveline constructions is shown in Figure 4

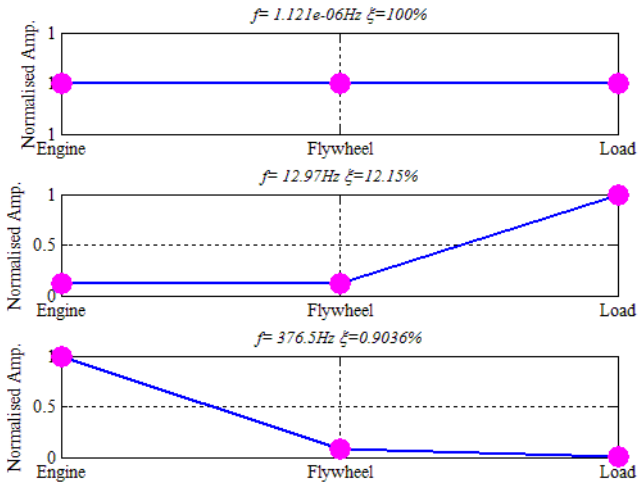

Figure 4 calculated mode shape and eigenfrequency

Results from calculated estimation using the engine's driveline parameters indicates that the system has three resonance frequency around 0Hz, 13Hz and 377Hz with only the 13Hz and 377Hz eigenfrequency showing a flexible mode of the system. While, the mode shape of the low frequency (13Hz) mode shows a high amplitude at the flywheel-load side, that of the high frequency (377Hz) mode shows high amplitude at the engine-flywheel side of the system.

D. Evaluation of IAS Based Stochastic Subspace Identification

Using pseudo random signal as the excitation vector, the response from the model assumed to be three encoder positions (front end, flywheel end and dyno end) were simulated. The frequency response of the system after excitation as shown in Figure 5 indicates frequency peaks around 13Hz and 377Hz. The amplitude of the peaks differs with the position of the response. While, the frequency peaks around the 13Hz shows a higher amplitude in the response from the dyno end compared to that from the front and flywheel end, the peaks around the 377Hz shows higher amplitude in the response from the front end of the system, low amplitude in that from flywheel end and no amplitude in the response from the load end of the system.

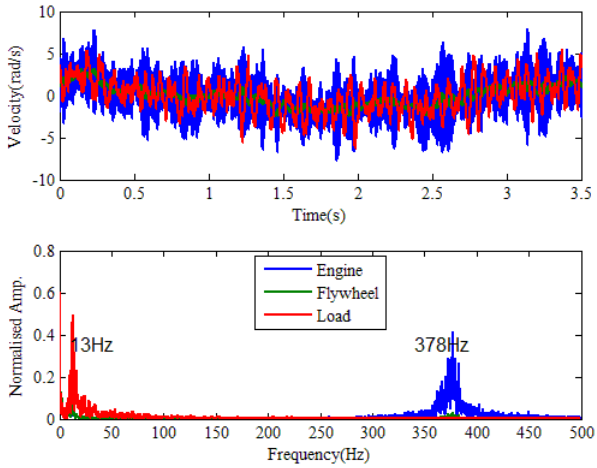

Figure 5 simulated response in time and frequency domain

The matrices A and C can be estimated either through a data-driven or covariance-driven stochastic subspace identification algorithm. In this paper the reference based correlation-driven SSI which is similar to the eigensystem realization algorithm (ERA) is adopted. See appendix A for details of the theoretical frameworks.

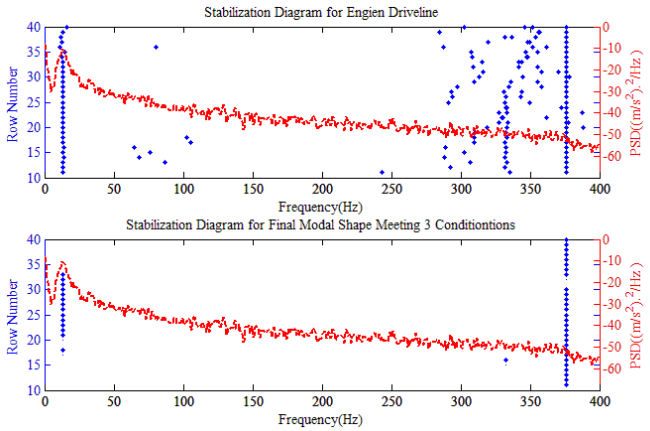

Figure 6 stabilization diagram from simulated response

Since, the true system order is unknown, for the simulated response, modal properties were calculated for increasing model orders of 10 to 40 as shown in Figure 6 above. In order to detect and remove modelled noise and weakly excited poles resulting from orders higher than the true system order, modal properties from different model orders were compared. And only those poles for which the relative difference in eigenfrequency, damping ratio and modal assurance criteria (MAC) is between certain values were used for modal property identification. The result indicates that two modes were stabilized in the frequency band from 0-400 Hz.

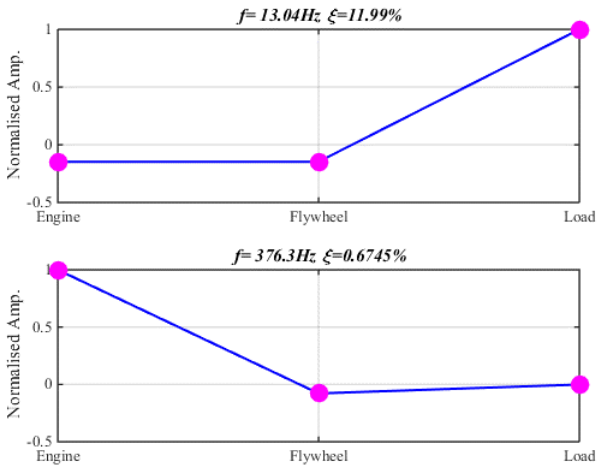

Figure 7 estimated mode shape from simulated response

Compared with that in Figure 4, the estimated mode shape and Eigen frequency for each mode using this SSI approach are very agreeable with the theoretical prediction value. However, the damping ratio tends to be slightly lower for the second mode, which may due to errors in numerical calculations

Table 2 summarizes the difference of modal parameters between the predicted and identified.

Table 2 compares estimated modal parameters with actual values

Mode	**Damping ratio (%)**			**Frequency (Hz)**		
	Actual value	**Estimated value**	**Δ%**	**Actual value**	**Estimated value**	**Δ%**
1	12.15	11.99	1.32	12.97	13.04	5.40
2	0.90	0.67	25.56	376.50	376.30	0.05

III. Experimental Evaluation

In order to carry out an IAS based modal property identification, a four-cylinder, four-stroke, turbocharged, direct injection diesel engine was used for experimental study.

A. System description and measurement

The test rig is fully equipped for in-cylinder pressure, IAS, emission and vibro-acoustics measurements. However, for this investigation the IAS measurement is the main focus. The IAS was measured from three locations (front end and flywheel end of the engine and the dynamometer end) using three different types of angular displacement measuring devices as shown in Figure 8. At the front end two optical switches are placed perpendicular to a circular disk with 180 holes. The circular disc is mounted concentric to the pulley which is mounted on the extruding shaft from the crankshaft. One optical switch measures one pulse per revolution while the other measure multi-pulse per revolution. At the flywheel side an MPU pick sensors is mounted at equidistant from the ring gear on the flywheel. While at the dynamometer end an incremental encoder was installed. See Table 2 for the encoder specifications.

TABLE 3 ENCODER SPECIFICATIONS

Encoder type	Location	PPR
Optical switch	Pulley (engine front end)	180
Magnetic pick-up	Flywheel	122
Incremental encode	Dynamometer	1024

See Figure 8 for the schematic view of the measurement system.

Using the event trigger option of the Sinocera data acquisition system and the one pulse per revolution signal as the trigger, the angular displacement of the engine driveline was sampled at a sampling frequency of 750 kHz during transient shut-down operation of the engine. The test was repeated under the same condition for ten times.

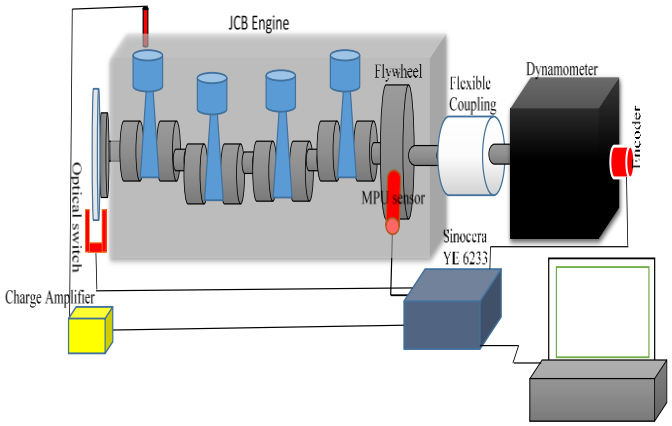

Figure 8 schematic diagram of the measurement system

B. Experimental Results and Discussion

Based on measured responses of IAS during engine shutdown operation, modal properties were calculated using the SSI approach. Figure 9, shows the stabilization diagram varying with increments of the row numbers of the data matrix.

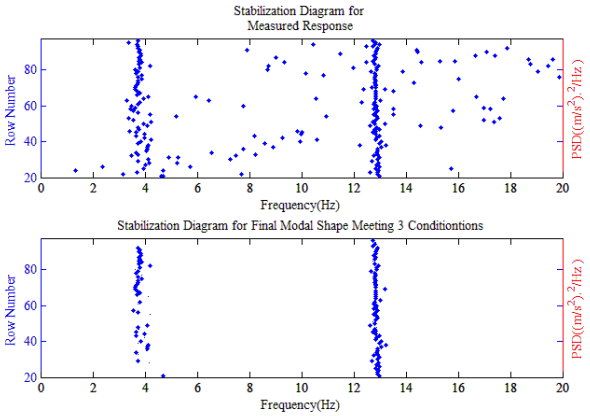

Figure 9 stabilization diagram for measured response

Result from the stabilization diagram shows two stable eigenfrequency in the frequency band from 0-20Hz, which is of interest for IAS analysis. The estimated shapes, eigenfrequency and damping ratio are shown in the figure 10.

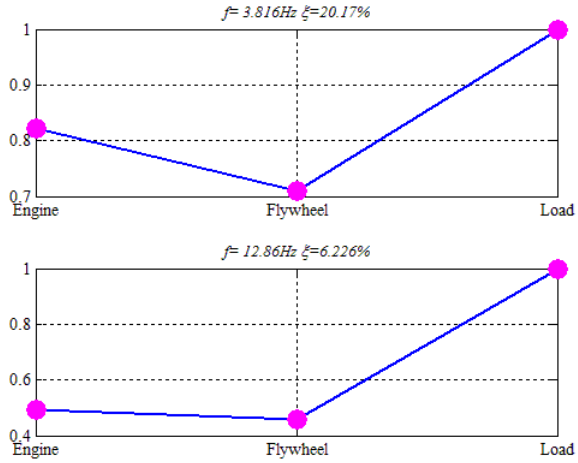

Figure 10 estimated mode shape from measured response

The identified frequency of 12.9Hz and its modal shape is agreeable with that from both calculated and simulated responses. But the damping ratio is lower, compared with the theoretical value. The result of the measured responses was unable to identify the high frequency mode (377Hz). This is because the excitation frequency range, which the engine sweeps through during transient shutdown is below this frequency mode. However, another low frequency component at 4Hz, which was not identified in the theoretical calculations and simulated responses was identified. This may be from the engine's body vibration because the encoder's transducer is fixed to the body of the engine.

IV. CONCLUSION

Based on the online output of angular speed SSI techniques allows modal properties of the engine driveline to be identified. In the low frequency range (<20Hz), only one significant mode at 12.9Hz has been extracted by using the SSI approach with three IAS measurements at the front end, flywheel end and dyno end respectively, which is agreeable with model prediction and hence shows the effectiveness of SSI based identification techniques.

Meanwhile, a potential component at 4.197Hz is also observed in the measurement, which may be due to the effect of body vibration due to asymmetrical dynamic interactions between the 4 cylinders. Nevertheless, this later component can be useful for engine misfire diagnosis.

REFERENCE

[1] Chen, S. K and Chang, .T, (1986), "Crankshaft torsional and damping simulation—an update and correlation with test results," SAE Paper, 95(4), pp.964-985.

[2] Juang, J. N. "Applied System Identification", Prentice Hall, Englewood Cliffs, NewJersey, 1994.

[3] Overschee. V. P., and De Moor. B., (1996), "Subspace Identification for Linear Systems", Kluver Academic Publishers.

[4] Moller. N., Brinker. R., and Anderson. P., (2000) "Modal Extraction on a Diesel Engine in Operation", Proc. of the 18th International Modal Analysis Conference, San Antonio, Texas

[5] Yang. J., Pu. L., Wang. Z., Zhou. Y., and Yan. X., (2000)," Fault Detection in a Diesel Engine by Analysing the Instantaneous Angular Speed", Mechanical Systems and Signal Processing 15(3), 549-564K. Elissa, "Title of paper if known," unpublished.

[6] Brincker. R. (2014) "Some Elements of Operational Modal Analysis", Hindawi Publishing Corporation Shock and Vibration

[7] Rangwala. A. S., (2001),"Reciprocating Machinery Dynamics, Design and Analysis". Marcel Dekker, Inc.

[8] Schagerberg. S and McKelvey. T., (2003), "Instantaneous Crankshaft Torque Measurements – Modelling and Validation", Society of Automotive Engineering, 2003-01-0713.

[9] Marty. A. J., and Plint. M. A., (2011), "Engine Testing: Theory and Practice", Elsevier 3ed.

[10] Brincker. R., and Ventura. C. E., (2015), "Introduction to Operational Modal Analysis", John Wiley & Sons.

[11] Peeters. B., and Roeck. G., (1999), "Reference-Based Stochastic Subspace Identification for Output-only Modal Analysis", Mechanical Systems and Signal Processing, 13(6), pp855-878

[12] Williams, .J. (1996), 'An Overview of Misfiring Cylinder Engine Diagnostic Techniques Based on Crankshaft Angular Velocity Measurements', SAE International in Proc. of SAE International Congress and Exposition, Detroit, USA,pp.31-37.

[13] Gawande, S. H., Navale, L. G., Nandgaonkar, M. R., Butala, D. S. and Kunamalla, S, (2010),' Detecting Power Imbalance in Multi-Cylinder Inline Diesel Engine Genset', Journal of Electronic Science and Technology, 8(3), pp.273-279.

[14] Chen, S. K and Chang, .T, (1986), "Crankshaft torsional and damping simulation—an update and correlation with test results," SAE Paper, 95(4) pp. pp.964-985.

[15] Citron, S. J., Higgins, E.O. and Chen, Y. (1989),'Cylinder by Cylinder Engine Pressure and Pressure Torque Waveform Determination Utilizing Speed Fluctuations 'International Congress and Exposition

[16] Taraza, D., and Henein, N.A., 1998, "Determination of the Gas-Pressure Torque of a Multi-cylinder Engine from Measurements of the Crankshaft's Speed Variation", SAE Technical Paper 980164.

Appendix A

In output only modal analysis of linear and time-invariant physical system, the parametric model structure for a stochastic state space system is given as: [3 11]:

$$x_{k+1} = Ax_k + w_k$$
$$y_k = Cx_k + v_k \quad (7)$$

With, w_k and v_k having zero mean, $E[w_k] = 0$ $E[v_k] = 0$ and the covariance matrices given by (6) the stochastic process is assumed to be stationary with zero mean $E[x_k \quad x_k^T] = \Sigma, E[x_k] = 0$ where Σ is the state covariance matrix and is independent of time k [2, 3, 11].

The output covariance matrices are defined as:

$$\Lambda_i = \mathrm{E}[y_{k+i} \quad y_k^T] \quad (8)$$

The next state-output covariance matrix G is defined as

$$G = E[x_{k+1} \quad y_k^T] \quad (9)$$

These definitions results to the deduction of the following properties [2, 11]:

$$\Sigma = A\Sigma A^T + Q$$
$$\Lambda_0 = C\Sigma C^T + R \quad (10)$$
$$\mathrm{G} = A\Sigma C^T + S$$

$$\Lambda_i = CA^{i-1}G \quad (11)$$

According to Peeters and Roeck [11] equation (11) is very essential and implies that covariance of outputs can be considered as impulse responses of the deterministic linear time-invariant A, G, C, Λ_0.

While there are two main types of SSI formulations, which are, the correlation and the data driven ones [10], in this paper the reference based correlation-driven SSI which is similar to the eigensystem realization algorithm (ERA) is adopted.

To implement this formulation the concept of reference output is explained.

Reference output are sensors which are placed at optimal locations on the structure where it is expected that all modes of vibration are present in the measured data [11].

Assuming that l elements of outputs are arranged so as to have r references first; then we have

$$y_t \equiv \begin{bmatrix} y_t^{ref} \\ y^{\sim ref} \end{bmatrix}, y_t^{ref} = Ly_t, L \equiv [I_r \quad 0] \quad (12)$$

y_t^{ref}, is reference output

$y^{\sim ref}$, is other output

L, is selection matrix that selects the references

The output measurements are gathered in a block Hankel matrix (a matrix where each diagonal consists of the repetition of the same element) with $2i$ block rows and j columns [11]. The first i blocks have r rows, the last i have l rows.

It is generally assumed that $j \to \infty$

$$\begin{bmatrix} y_0^{ref} & y_1^{ref} & \cdot & y_{j-1}^{ref} \\ y_1^{ref} & y_2^{ref} & \cdot & y_j^{ref} \\ \cdot & \cdot & \cdot & \cdot \\ y_{i-1}^{ref} & y_i^{ref} & \cdot & y_{i+j-2}^{ref} \\ \hline y_i & y_{i+1} & \cdot & y_{i+j-1} \\ y_{i+1} & y_{i+2} & \cdot & y_{i+j} \\ \cdot & \cdot & \cdot & \cdot \\ y_{2i-1} & y_{2i} & \cdot & y_{2i+j-2} \end{bmatrix} \equiv \begin{bmatrix} Y_{0|i-1}^{ref} \\ \hline Y_{i|2i-1} \end{bmatrix} \quad (13)$$

Notice the output data is scaled by a factor of $1/\sqrt{j}$. The subscript p and f stands for past and future

By splitting H into two parts of i block rows the, matrices Y_p^{ref} and Y_f are defined.

The extended observability matrix is defined as:

$$O_i = \begin{bmatrix} C \\ CA \\ CA^2 \\ \cdots \\ CA^{i-1} \end{bmatrix} \quad (14)$$

It is assumed that the matrix pair$\{A, C\}$ is observable, meaning all the dynamic modes of the system can be observed in the output

The reference reversed extended stochastic controllability matrix is

$$C_i^{ref} \equiv [A^{i-1} \quad G^{ref} \quad A^{i-21}G^{ref} \quad \cdots \quad AG^{ref} \quad G^{ref}] \quad (15)$$

This method only needs the covariance between the outputs and a limited set of reference outputs instead of the covariance between all outputs. The covariance output using equation (10) is defined as:

$$\Lambda_i = E\left[y_{t+i}\, y_t^{ref^T}\right] \quad (16)$$

The next state-reference output covariance is

$$G^{ref} \equiv E\left[x_{t+1} \quad y_t^{ref^T}\right] = GL^T \quad (17)$$

This then leads to the second relation in (13)

$$\Lambda_i^{ref} = CA^{i-1}G^{ref} \quad (18)$$

The covariance are then gathered in a block Toeplitz matrix where each diagonal consist of the repetition of the same element

$$T_{1|i}^{ref} \equiv \begin{bmatrix} \Lambda_i^{ref} & \Lambda_{i-1}^{ref} & . & \Lambda_1^{ref} \\ \Lambda_{i+1}^{ref} & \Lambda_i^{ref} & . & \Lambda_2^{ref} \\ . & . & . & . \\ \Lambda_{2i-1}^{ref} & \Lambda_{2i-2}^{ref} & . & \Lambda_i^{ref} \end{bmatrix} \quad (19)$$

From (16) and assuming ergodicity, the block Toeplitz matrix yields

$$T_{1|i}^{ref} = Y_f Y_p^T \quad (20)$$

Due to equation (18) the block Toeplitz matrix decomposes as

$$T_{1|i}^{ref} = \begin{bmatrix} C \\ CA \\ \cdots \\ CA^{i-1} \end{bmatrix} [A^{i-1} \quad G^{ref} \quad A^{i-21}G^{ref} \quad \cdots \quad AG^{ref} \quad G^{ref}] = O_i C_i^{ref} \quad (21)$$

The observability and reference-reversed controllability matrix, can be obtained by applying the singular-value decomposition (SVD) to the block Toeplitz matrix [11]:

$$T_{1|i}^{ref} = USV^T = [U_1 \quad U_2] \begin{bmatrix} S_1 & 0 \\ 0 & 0 \end{bmatrix} \begin{bmatrix} V_1^T \\ V_2^T \end{bmatrix} = U_1 S_1 V_1^T \quad (22)$$

Where U and V are orthonormal matrices $U^TU = UU^T = I_{li}$ and $V^TV = VV^T = I_{ri}$ and S is a diagonal matrix containing the singular values in descending order.

Since the inner dimension of the product $O_i C_i^{ref}$ equal n and since we assume that$ri \geq n$, the rank of the product cannot exceed n.

The rank of a matrix is found as the number of non-zero singular values. In the last equality of equation (22), the zero singular values and corresponding singular vectors are omitted. With equations (21) and (22), we can now state that

$$O_i = U_1 S_1^{1/2}$$
$$C_i^{ref} = S_1^{1/2} V_1^T \quad (23)$$

The solution to the identification problem is straightforward, once O_i and C_i^{ref} are known

From equation (14) and (15) we can say that C equals the first l rows of O_i and G_{ref} equals the last r columns of C_i^{ref}. The state matrix A can be found by decomposing a shifted block Toeplitz matrix:

$$T_{2|i+1}^{ref} = O_i A C_i^{ref} \quad (24)$$

By solving equation (27) for A yields

$$A = O_i^{\dagger}\ T_{2|i+1}^{ref} C_i^{ref^{\dagger}} \quad (25)$$

The symbol $(\blacksquare)^{\dagger}$ represent the pseudo-inverse of a matrix.

After identifying the discrete state matrix, the modal parameters can be estimated since the dynamic behaviour of the system is completely characterised by its eigenvalues:

$$A = \Psi \Lambda \Psi^{-1} \quad (26)$$

$\Lambda = \text{diag}[\lambda_q]$, is a diagonal matrix containing the discrete-time complex eigenvalues Ψ, contains the eigenvectors as columns.

The continuous time state equation (2) is equivalent to the second-order matrix equation of motion (1).

Consequently, they have the same eigenvalues and eigenvectors. These can be obtained by an eigenvalue decomposition of the continuous-time state matrix:

$$A_c = \Psi_c \Lambda_c \Psi_c^{-1} \quad (27)$$

$\Lambda_c = \text{diag}\left[\lambda_{c_q}\right]$, is a diagonal matrix containing the continuous-time complex eigenvalues

Ψ_c, contains the eigenvectors as columns

As a result of the equation (4)

$$A = exp(A_c \Delta t) \quad (28)$$

Which will yield

$$\Psi_c = \Psi, \lambda_{c_q} = \frac{\ln(\lambda_q)}{\Delta t} \quad (29)$$

The eigenvalues of $A_c$occurs in a complex conjugated pairs can be written as

$$\lambda_{c_q}, \lambda_{c_q}^* = -\xi_q \omega_q \pm j\omega_q \sqrt{1 - \xi_q^2} \quad (30)$$

ξ_q, is the modal damping ratio of mode q and $\omega_q$is the eigenfrequency of mode q (rad/s).

The mode shapes at the sensor locations defined as columns Φ_q of Φ are the observed parts of the system eigenvectors Ψ are thus obtained using the observation equation (5)

$$\Phi = C\Psi \quad (31)$$